Anal. Chem. **2000,** *72,* 333−338

Spatially Addressed Deposition and Imaging of Biochemically Active Bead Microstructures by Scanning Electrochemical Microscopy

C. Ajith Wijayawardhana,[†,‡,§] Gunther Wittstock,[*,†] H. Brian Halsall,[‡] and William R. Heineman[‡]

University of Leipzig, Wilhelm Ostwald Institute of Physical and Theoretical Chemistry, Linnéstrasse 2, D-04103 Leipzig, Germany, and University of Cincinnati, Department of Chemistry, Cincinnati, Ohio 45221-0172

A new procedure is described to deposit paramagnetic beads on surfaces to form microscopic agglomerates. By using surface-modified beads, microscopic structures with defined biochemical activity are formed. The shape and size of agglomerates were characterized by scanning electron microscopy (SEM), and the biochemical activity was mapped with scanning electrochemical microscopy (SECM). This approach is demonstrated using beads modified with anti-mouse antibodies (Ab). After allowing them to react with a conjugate of mouse IgG and alkaline phosphatase (ALP), the beads were deposited as agglomerates of well-defined size and shape. The biochemical activity was recorded in the generation−collection SECM mode by oxidizing 4-aminophenol formed in the ALP-catalyzed hydrolysis of 4-aminophenyl phosphate at the surface of the beads. The signal height correlated with both the amount of beads present in one agglomerate and the proportion of Ab binding sites saturated with the ALP−mouse IgG conjugate. The feedback mode of the SECM was used to image streptavidin-coated beads after reaction with biotinylated glucose oxidase.

Intensive research efforts to immobilize biomolecules in microscopic domains on solid surfaces are stimulated by several prospective new applications[1] and the improvement of existing assay technologies.[2,3] The requirement to minimize the sample volume extends beyond special applications, such as clinical testing of neonates or the analysis of precious archived specimens, to clinical testing, in general, as regulatory agencies in the US call for an increased awareness of clinical labs to the importance of drawing a minimum amount of blood from critically injured or ill patients.[4] The trend to high-throughput screening adds an additional impetus to develop technologies to process many samples simultaneously and rapidly.[5] In the case of heterogeneous assays this goal is approached best if microscopic sensitive regions are present on a single support and exposed to small amounts of liquid samples. Alternatively, several analytes within one sample can be analyzed simultaneously on a surface having different sensitive regions. Miniaturization brings additional advantages for assays using enzyme-labeling in conjunction with amperometric or voltammetric detection schemes. These techniques determine a solute concentration, and thus reducing the ratio between detection volume and sensitive surface area increases the sensitivity and improves the detection limit. Sensors or assays where the biocomponent is immobilized directly onto the detecting electrode generally face the problem that the protein coating inhibits the heterogeneous electron transfer by blocking the electrode surface. Ratcliff et al.[7] introduced the concept of microcompartmentalization by preparing microheterogeneous electrode surfaces with microscopic blank regions for the electrochemical reactions and others that serve as a solid support for the biomolecules. The popularity of the approach is illustrated by very recent reports that use interference patterns[8] or local electrochemical precursor generation[9] to form the microcompartmentalized heterogeneous surfaces.

Biochemically active layers can be patterned by ink-jet technology,[10] screen printing,[11] photoresist/lift-off methodology,[12] microcontact printing,[13,14] local photochemical activation of a preimmobilized coupling agent,[15−17] or local electropolymerization of polymer, onto which enzymes are coupled in a second step.[18]

* To whom correspondence should be directed: Fax (+49-341) 97 36399; Email wittstoc@rz.uni-leipzig.de.

† University of Leipzig.

‡ University of Cincinnati.

§ Graduate student of the University of Cincinnati and visiting student at the University of Leipzig

(1) Kricka, L. J. *Clin. Chem.* **1998**, *44*, 2008−2014.
(2) Ekins, R. P.; Chu, F. W. *Clin. Chem.* **1991**, *37*, 1955−1967.
(3) Ekins, R. P. *Clin. Chem.* **1998**, *44*, 2015−2030.
(4) Wittstock, G.; Jenkins, S. H.; Halsall, H. B.; Heineman, W. R. *Nanobiology* **1998**, *4*, 153−162.
(5) Silzel, J. W.; Cercek, B.; Dodspon, C.; Tsay, T.; Obremski, R. J. *Clin. Chem.* **1998**, *44*, 2036−2043.
(6) Cousino, M. A.; Jarbawi, T. B.; Halsall, H. B.; Heineman, W. R. *Anal. Chem.* **1997**, *69*, 544A−549A.
(7) Ratcliff, B. B.; Klancke, J. W.; Koppang, M. D.; Engstrom, R. C. *Anal. Chem.* **1996**, *68*, 2010−2014.
(8) Dontha, N.; Nowall, W. B.; Kuhr, W. G. *Anal. Chem.* **1997**, *69*, 2619−2625.
(9) Nowall, W. B.; Wipf, D. O.; Kuhr, W. G. *Anal. Chem.* **1998**, *70*, 2601-2606.
(10) Newman, J. D.; Turner, A. F. P.; Marrazza, G. *Anal. Chim. Acta* **1992**, *262*, 13−17.
(11) Hart, J. P.; Wring, S. A. *Electroanalysis* **1994**, *6*, 617−624.
(12) Connolly, P. *TIBTECH* **1994**, *12*, 123−127.
(13) Bernard, A.; Delamarche, E.; Schmidt, H.; Michel, B.; Bosshard, H. R.; Biebuyck, H. *Langmuir* **1998**, *14*, 2225−2229.
(14) Lahiri, J.; Ostuni, E.; Whitesides, G. M. *Langmuir* **1999**, *15*(5), 2055−2060.
(15) Pritchard, D. J.; Morgan, H.; Cooper, J. M. *Anal. Chem.* **1995**, *67*, 3605−3607.
(16) Pritchard, D. J.; Morgan, H.; Cooper, J. M. *Angew. Chem., Int. Ed. Engl.* **1995**, *34*, 91−93.
(17) Bhatia, S. K.; Teixeira, J. L.; Anderson, M.; Shriver-Lake, L. C.; Calvert, J. M.; Georger, J. H.; Hickman, J. J.; Dulcey, C. S.; Shoen, P. E.; Ligler, F. S. *Anal. Biochem.* **1993**, *208*, 197−205.

10.1021/ac990977q CCC: $19.00
Published on Web 12/11/1999

Scanning electrochemical microscopy (SECM)[19,20] has become a powerful tool to image localized biochemical activity on modified surfaces. Two major modes of operation can be distinguished. In the feedback mode the ultramicroelectrode probe produces an artificial electron acceptor or donor for an oxidoreductase. The enzymatic reaction regenerates the original mediator and enhances the current above enzymatically active regions. This mode was first applied with glucose oxidase (GOx), for which ferrocinium ions or ferricyanide act as electron acceptors.[21,22] Alternatively, the microelectrode can collect any redox-active species generated by an enzymatic reaction at the sample surface (generation−collection (GC) mode).[23] Antibodies have been visualized after labeling them with antigen−enzyme conjugates.[24] Shiku et al.[25] used SECM to resolve antibody-modified spots and were able to test for the same analyte in different samples[26] and determine different analytes in one sample.[27]

SECM can be used to pattern the surface and to image the resulting heterogeneous distribution of biochemical activity with the same instrument, and this has been exploited in a number of studies aiming to understand and improve the detection of very small quantities of immobilized material.[18,28] It soon became clear that the sensitivity of the SECM detection in the generation−collection mode is very high because the microelectrode and its insulating shielding form a leaking thin-layer cell with the specimen surface. In such a situation, the dilution of the products of the enzymatic reaction is slowed. If the active region itself extends below 50 μm, a steady-state diffusion layer can be expected which is an advantage for analytical determinations.

In this paper we report a novel method for generating biochemically active sites of micrometer dimensions onto surfaces and their imaging in the GC and feedback modes of SECM. The sites consist of a predetermined quantity of paramagnetic immunobeads assembled as small mounds. They were characterized by SEM and SECM.

EXPERIMENTAL SECTION

Chemicals and Bead Modifications. Twenty μL of a magnetic bead suspension coated with antimouse antibodies (Ab) (mean diameter 2.8 μm, Dynal, Great Neck, NY) were incubated for 45 min with 3 μL of a solution of 11.4 mg mL^{-1} Chrompure mouse IgG as antigen (Ag) conjugated to alkaline phosphatase (Jackson Immunoresearch Laboratory, West Grove, PA) in Tris buffer (pH 9).

Streptavidin-coated beads (10 μL suspension mean diameter 1 μm, Bangs Laboratories, Fishers, IN) were allowed to react for 45 min with 1000 μL of a solution of 0.005 mg mL^{-1} biotinylated GOx (Vector Laboratories, Burlingame, CA) in 0.05 M acetate buffer (pH 4.5). In both cases, rinsing was done with the buffer solution containing 0.25% Tween 20 (Sigma, Deisenhofen, Germany).

Immunobeads were detected by SECM using a solution of disodium 4-aminophenyl phosphate (PAPP) synthesized according to ref 29 in Tris buffer (4 mM PAPP, 1 g L^{-1} $MgCl_2$, 0.1 M KCl, 0.02% NaN_3, 0.1 M Tris-HCl, pH 9.0). The solution was deoxygenated and measurements carried out in the dark to minimize the decomposition of PAPP.

GOx was detected using a deoxygenated solution of 50 mM glucose (Fluka, Buchs, Switzerland) and 1 mM dimethylaminomethyl ferrocene (DMAMFc, ABCR GmbH, Karlsruhe, Germany) in phosphate buffer (pH 6.9).

Microspotting the Magnetic Beads. Surface-modified magnetic beads were allowed to react with ALP-labeled mouse IgG or biotinylated GOx. These procedures were simplified as the suspensions can be mixed easily with the reactants while a simple rare earth permanent magnet is sufficient to retain the magnetic beads against the test tube wall while pouring off the supernatant liquid. The bead suspension was brought to the desired dilution, determined previously for the different bead preparations. One microliter of the bead suspension was taken up in a variable volume micropipet (Gilson Microman Bio M-10, 0.5−10 μL, Villiers-le-Bel, France or Eppendorf Research, 0.1−2.5 μL, Eppendorf GmbH, Hamburg, Germany). The tip of the micropipet was mounted in the electrode holder of the SECM translation stage. The support onto which the beads were to be deposited was mounted on a permanent rare earth magnet. The support surfaces need to be hydrophobic, and this was achieved by covering glass with stretched Parafilm "M" (American National Can, Chicago, IL) or silanizing glass slides with octadecyltrichlorosilane (Fluka). A drop of 0.9 μL bead suspension was extruded from the micropipet by reducing the volume selection of the pipet from 1 μL to 0.1 μL. The drop was held for about 30 s at 500 μm above the support surface (Figure 1a), when the beads are drawn magnetically to the bottom of the drop. Reducing the drop size to 0.3 μL then helps to focus the beads (Figure 1b). This reduced drop was brought into contact with the hydrophobic support (8 μm s^{-1} just before contact). After observing, visually, the contact of the liquid with the hydrophobic surface (Figure 1c), the direction of motion was reversed (8 μm s^{-1}). The drop adheres to the retracting micropipet tip, and the liquid is removed almost completely from the support surface while the magnetic beads are retained on the surface (Figure 1d).

Instrumentation and Imaging. SECM measurements were taken on two home-built instruments. One system[30] uses Inchworm actuators (Burleigh Inc., Fishers, NJ) and a home-built bipotentiostat. The other system is based on stepper motors and control electronics allowing 0.01 μm incremental motion (Scientific Precision Instruments, Inc., Oppenheim, Germany), and a bipotentiostat PG10 (Jaissle Elektronik, Waiblingen, Germany). Further details of the second system are available upon request. The

(18) Kranz, C.; Wittstock, G.; Wohlschläger, H.; Schuhmann, W. *Electrochim. Acta* **1997**, *42*, 3105−3111.
(19) Bard, A. J.; Fan, F.-R. F.; Pierce, D. T.; Unwin, P. R.; Wipf, D. O.; Zhou, F. *Science* (*Washington, D.C.*) **1991**, *254*, 68−74.
(20) Mirkin, M. V. *Mikrochim. Acta* **1999**, *130*, 127−153.
(21) Pierce, D. T.; Unwin, P. R.; Bard, A. J. *Anal. Chem.* **1992**, *64*, 1795−1804.
(22) Pierce, D. T.; Bard, A. J. *Anal. Chem.* **1993**, *65*, 3598−3604.
(23) Horrocks, B. J.; Schmidtke, D.; Heller, A.; Bard, A. J. *Anal. Chem.* **1993**, *65*, 3605−3614.
(24) Wittstock, G.; Yu, K.; Halsall, H. B.; Ridgway, T. H.; Heineman, W. R. *Anal. Chem.* **1995**, *67*, 3578−3582.
(25) Shiku, H.; Hara, Y.; Takeda, T.; Matsue, T. Uchida, I. in *Solid−Liquid Electrochemical Interfaces*; Jerkiewicz, G., Soriaga, M. P., Uosaki, K., Wieckowski, A. Eds.; ACS Symposium Series 656; American Chemical Society: Washington, DC, 1997; Chapter 15.
(26) Shiku, H.; Matsue, T.; Uchida, I. *Anal. Chem.* **1996**, *68*, 1276−1278.
(27) Shiku, H.; Hara, Y.; Matsue, T.; Uchida, I.; Yamauchi, T. *J. Electroanal. Chem.* **1997**, *438*, 187−190.
(28) Wittstock, G.; Schuhmann, W. *Anal. Chem.* **1997**, *69*, 5059−5066.
(29) DeRiemer, L. H.; Meares, C. F. *Biochemistry* **1981**, *20*, 1606−1612.
(30) Wittstock, G.; Emons, H.; Ridgway, T. H.; Blubaugh, E. A.; Heineman, W. R. *Anal. Chim. Acta* **1994**, *298*, 285−302.

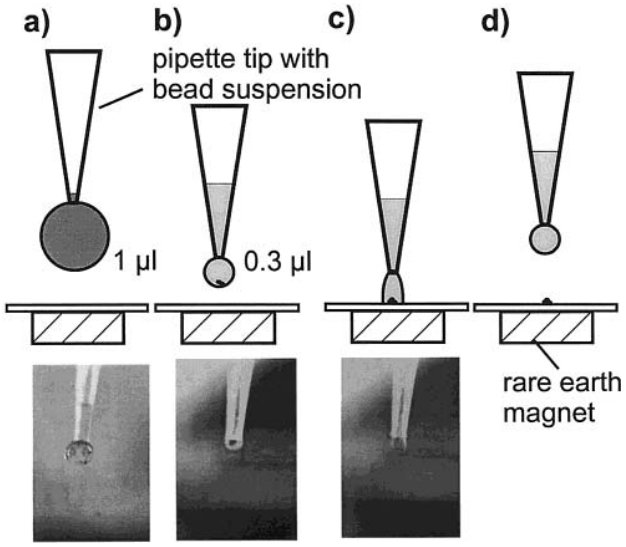

Figure 1. Schematic representation of the bead-deposition protocol and images obtained with a CCD camera. (a) Drop of bead suspension is extruded out of the micropipet, (b) after concentrating the beads in the drop tip, the drop size is reduced to 0.3 μL, (c) the drop is set on the hydrophobic surface, d) the drop will stay at the pipet tip if the pipet is retracted slowly from the surface, leaving the beads behind.

electrochemical three-electrode cell consisted of a silver wire as quasi-reference electrode or a saturated calomel electrode (EG&G, Munich, Germany), a Pt wire as auxiliary electrode, and a Pt microdisk electrode made from 10-μm-diameter wire sealed in glass and beveled according to ref 31. The microelectrode was held at +290 mV to detect 4-aminophenol (PAP) in GC experiments and at +400 mV to oxidize DMAMFc in feedback experiments. The horizontal translation rate was 8 μm s^{-1}. The microelectrode was positioned above the surface by moving the microelectrode perpendicularly toward the sample (0.7 μm s^{-1}) while monitoring the negative feedback during O_2 reduction and DMAMFc oxidation. For GC experiments, the electrode was removed about 45 μm from the surface. Before feedback experiments, the approach of the microelectrode toward the surface was performed in a lateral distance of several hundred micrometers to the deposited bead agglomerates and retracted 25 μm from the glass surface. Estimating the height of the bead agglomerations from Figure 2b as 12−23 μm, the working distance measured to the top of the agglomerate was 2−13 μm. Scanning electron micrographs were acquired in a DSM 940 (Zeiss, Oberkochen, Germany) after sputter-coating the polymer beads with gold.

RESULTS AND DISCUSSION

The deposition procedure leads to a well-defined deposition of magnetic beads. Their three-dimensional arrangement can be imaged by SEM after coating the beads and the support with gold. Figure 2 shows SEM images of bead agglomerations deposited from suspension. As can be seen in the CCD image of Figure 1c, the droplet wets a circular area with a radius that corresponds to the radius r of the deposited droplet ($r \approx 500$ μm, shape assumed hemispherical). Nevertheless, the size of the bead agglomeration is determined primarily by the number of beads in the droplet (Figure 2), and the radii of the bead agglomerations are only 0.04−0.3 times the radius of the wetted area. This is due to the paramagnetic properties of beads and the lateral flow of liquid during the retraction of the micropipet. The height of the bead agglomerates cannot be determined accurately from SEM images even when imaged under a tilt angle. The height of the agglomerates also exceeds the vertical positioning range of the AFM scanners available in the department (x, y, 100 μm; z, 6 μm). For the SEM images in Figure 2a,b the maximum tilt angle α of 45 ° available at our setup was used. A rough estimate of the height of the agglomerates can be attempted when the bead laying on top of the agglomerate can be identified and is situated above the diameter parallel to the horizontal image frame (Figure 2d). The height h is then projected onto the paper plane with an angle $\alpha = 45°$ where it gives a projection $h' = h \sin \alpha$. Selecting the bead laying on top of the agglomeration is not straightforward, and the height of the agglomeration in Figure 2a is therefore an estimate at (120 ± 17) μm and that in Figure 2b at (18 ± 5) μm. The latter value corresponds to (9 ± 3) layers of beads assuming a hexagonal arrangement. Also note that the shape of the bead agglomeration changes as the bead number is decreased. While the shape in Figure 2a can be approximated by a hemisphere, it is only a part of a hemisphere in Figure 2b and apparently only two layers of beads in Figure 2c. This variation can be understood by considering the lateral force acting on an individual bead compared with the vertical magnetic force imposed by the permanent magnet. Assuming constant magnetic susceptibility, the lateral force will grow as the total number of beads contained in an agglomerate increases, eventually leading to agglomerates with shapes close to a hemisphere. When comparing agglomerates of constant bead numbers but from batches with different magnetic susceptibility, those of higher susceptibility will tend to arrange in agglomerates with larger height.

Thus, the size of the aggregated bead structure can be tuned by means of the concentration of the bead suspension used for deposition, while combining the micropipet with a micropositioning system gives free choice in their placement. Together, these features give maximum flexibility for prototyping tasks. The bead agglomerations are stable after drying and adhere to the support even without the presence of the permanent magnet. Depending on their biochemical modification, their activity can be restored by immersion in an appropriate buffer solution. The surface onto which the beads are deposited must be hydrophobic or the drop will not adhere to the pipet during retraction. Only the retraction of the drop generates the lateral flow necessary for assembling the beads in well-defined agglomerates. Because our electrodes are too hydrophilic, we did not attempt to assemble bead agglomerations directly on electrode surfaces and to record the production of PAP at the surface onto which the beads reside.

The biochemical activity of the deposited particles can be analyzed with SECM using a procedure similar to that of imaging an anti-digoxin Ab[24] immobilized on glass. The suspension of Ab-coated beads was incubated with the enzyme-labeled Ag (mouse IgG−ALP conjugate). After mounting the support with the bead agglomerate in an electrochemical cell containing PAPP, the ALP-generated product PAP was detected amperometrically by the microelectrode. PAP can be oxidized at potentials more positive

(31) Kranz, C.; Ludwig, M.; Gaub, H. E.; Schuhmann, W. *Adv. Mater.* (*Weinheim, Ger.*) **1995**, *7*, 38−40.

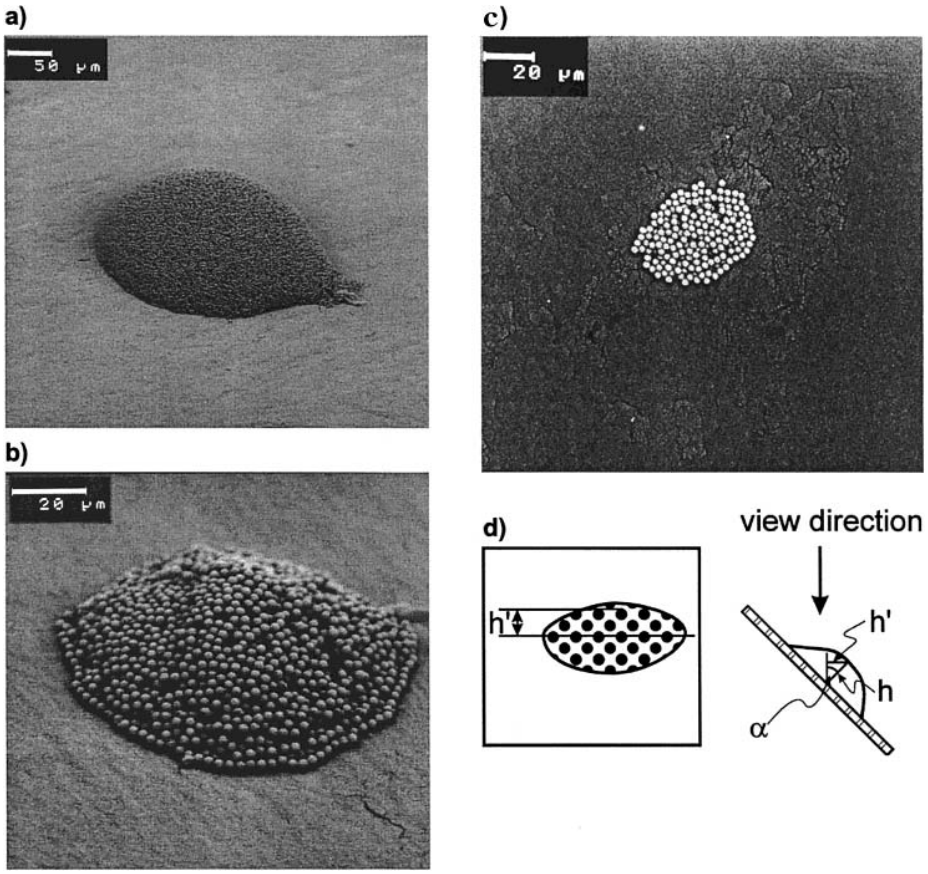

Figure 2. SEM images of deposited magnetic beads obtained after drying and Au-coating. The varied size of the deposited bead aggregates was achieved by varying the dilution of the bead suspension used for deposition. Particle concentration in the suspension in particles per milliliter: (a) 6.7×10^8, tilt angle 45°; (b) 6.8×10^6, tilt angle 45°; (c) 4.0×10^5, tilt angle 0°. (d) Determination of the approximate height of the agglomerations; (left) selecting the bead on top of the agglomerate in a SEM image, (right) calculation of *h*.

than 30 mV (vs Ag/AgCl), a potential where PAPP is not redoxactive. The details of the electrochemistry of PAPP and PAP have been investigated in detail by cyclic voltammetry.[32] Since then the system has been used in a number of bioanalytical applications. Figure 4 of ref 24 compares differential pulse voltammograms of PAP and PAPP.

Since the deposited bead agglomerates are themselves microstructures, a quasi stationary hemispherical diffusion layer of PAP develops. This enhances the possibilities for quantitation compared with the approach taken in ref 24.

For beads completely saturated with the Ag−ALP conjugate, the signal height in SECM images varies with the number of deposited beads (Figure 3). The lateral signal width in SECM images is much larger than the geometric extension of the agglomerations taken from corresponding SEM images (Figure 3). The detection limit is imposed by the sensitivity of the potentiostat (1 nA V^{-1}), and even smaller numbers of beads should be detectable with a more sensitive potentiostat.

For a given number of beads, the signal height depends on the amount of ALP captured via the reaction of anti-mouse Ab with the mouse IgG−ALP conjugate. Different signal heights in SECM images can be observed if constant numbers of beads are deposited that have different levels of saturation with mouse IgG-ALP conjugate. From previous experiments with rotating disk electrodes (RDE) it is known that the incubation of Ab-coated beads with a 10^2-fold dilution of the conjugate solution will give 30% of the signal obtained using the stock conjugate solution if all other parameters are kept constant. Accordingly, 20-μL aliquots of the stock suspension of Ab-coated beads were shaken with 3 μL of undiluted and 10^2-fold-diluted conjugate solutions. After rinsing and washing steps, the modified bead suspensions were brought to the same dilution by adding buffer. Deposition was done from these suspensions. The resulting SECM images of the beads treated with the diluted conjugate show a peak to baseline current of 1.3 nA compared to 2.1 nA obtained with beads completely saturated with the conjugate (Figure 4). The "assay" for the conjugate was not further optimized and it is difficult to estimate the detection limit as this would depend not only on the detection limit of the SECM readout but also on the binding properties of the immobilized antibody, on the absolute number of beads deposited as well on the on the number of beads exposed to a given sample volume. The advantage of a SECM readout compared to traditional enzyme immunoassays is the possibility of avoiding the incubation to produce PAP and to have several active regions on one support. It is, however, expected that better detection limits can be achieved in formats where PAP is generated in a microscopic volume and detected at interdigitated

(32) Tang, H. T.; Lunte, C. E.; Halsall, H. B.; Heineman, W. R. *Anal. Chim. Acta* **1988**, *214*, 187−195.

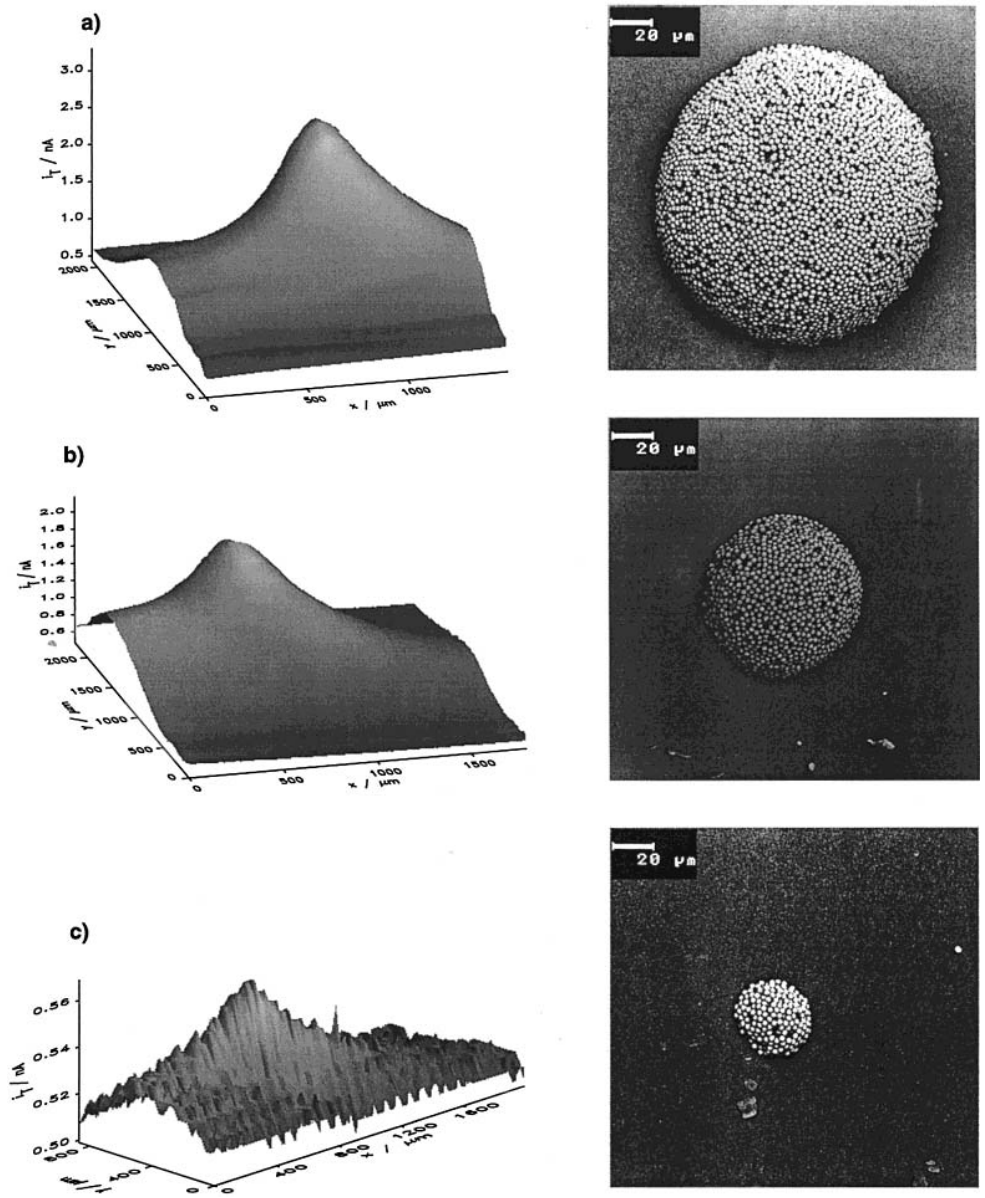

Figure 3. Series of SECM images of bead agglomerations. The beads were coated with anti-mouse Ab saturated with a conjugate of mouse IgG and alkaline phosphatase. The SECM images were obtained in the GC mode by oxidizing enzyme-generated PAP. SEM images of representative bead agglomerations illustrate the size of the deposits from which the SECM images were obtained. Particle concentration in the suspension in particles per milliliter: (a) 4.1×10^7, (b) 4.1×10^6, (c) 4.1×10^5.

array electrodes (IDAs) or RDE (e.g., a droplet sandwiched between the support and an IDA or a RDE).

As has been discussed extensively in previous communications, the GC mode is very sensitive, but offers a very limited spatial resolution,[24,28] and so the enzyme-mediated feedback mode was used as well.[21,22] For this purpose, streptavidin-coated beads were modified with biotinylated GOx and deposited as above. The resulting bead agglomerations were imaged in a deaerated solution of glucose and DMAMFc. The ferrocinium form of DMAMFc is a very efficient artificial electron acceptor for GOx[33] and is produced at the microelectrode. During the enzymatic reaction, the reduced form of the mediator is regenerated, and therefore, the microelectrode current will increase above regions with GOx activity. Since an insulating support was selected for this study, no superposition of feedback by the enzymatic reaction and by a heterogeneous electron-transfer reaction need be considered (as was in ref 28). In enzyme-mediated feedback mode, images of typical bead agglomerations are as small as 25 μm taken as full width at half-maximum (Figure 5). This is close to the size of the bead agglomerations taken from SEM images (Figure 2c). The successful imaging depends critically on the microelectrode−support distance because the product of the electrolysis at the microelectrode is an essential cofactor for the enzymatic reaction. The product of the enzymatic reaction is detected at the microelectrode on top of a background current caused by the electro-

(33) Cass, A. E. G.; Davis, G.; Francis, G. D.; Hill, H. A. O.; Aston, W. J.; Higgins, I. J.; Plotkin, E. V.; Scott, L. D. L.; Turner, A. P. F. *Anal. Chem.* **1984**, *56*, 667−671.

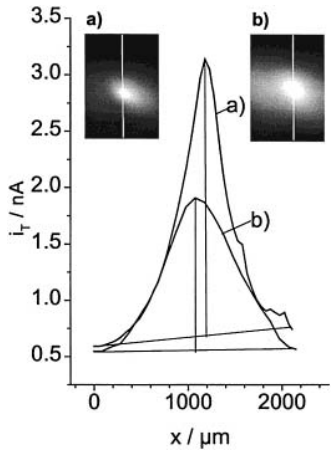

Figure 4. SECM images and profiles of bead agglomerations prepared from suspensions treated with different amounts of Ag-ALP conjugate. (a) 20 μl of a stock suspension of Ab-coated beads and 3 μL of Ag-ALP conjugate, (b) 20 μL of a stock suspension of Ab-coated beads and 3 μL of 10^2-fold diluted Ag-ALP conjugate. After washing, the suspensions were reconstituted by adding 200 μL of buffer. Deposition was done from 1 μL of these suspensions.

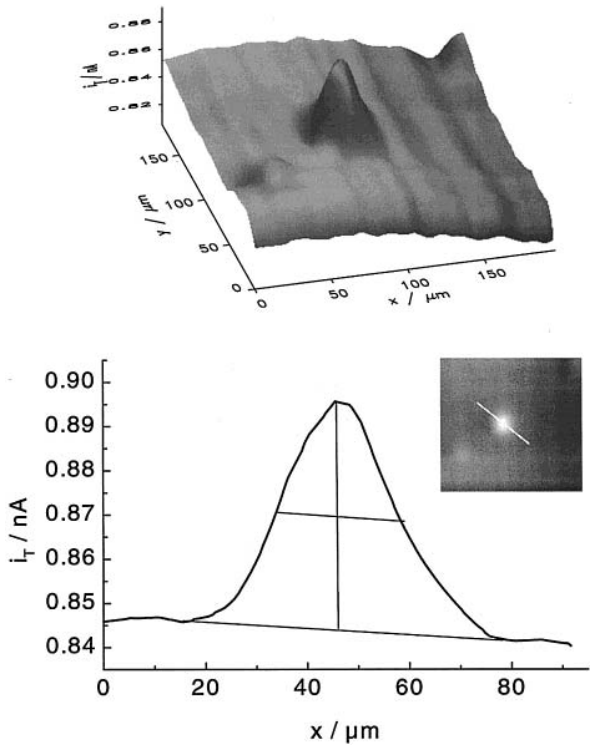

Figure 5. Feedback images of streptavidin-coated beads saturated with biotinylated GOx (a) with its cross section showing the signal width (b).

chemical conversion of the dissolved mediator to the cofactor. The combined effect of local cofactor generation and measurement of the electrochemical feedback on the background of the steady-state current controlled by hindered diffusion of the mediator toward the microelectrode leads to a comparatively sharp distance dependence in feedback images.[21,22] This is contrary to the situation in GC imaging in which all the substrates of the enzymatic reaction are contained in the bulk phase of the solution. The enzymatic reaction proceeds independently of the position of the microelectrode. The products of the enzymatic reaction spread out by diffusion. They are detected at the microelectrode on a low background because the solution bulk does not contain any redoxactive species. As the bead spots are larger than the microelectrode, the diffusion layer of the product of the enzymatic reaction will be larger than the diffusion field of the microelectrode, enabling the microelectrode to detect products diffusing away from the beads at a much larger distance than that required for current enhancement in a feedback experiment. In GC experiments under the condition of high enzymatic activity and low substrate concentration, the microelectrode may actually shield the enzymatically active region from the supply of reactant if the microelectrode−support distance becomes very small. An instructive approach curve of this type is discussed in Figure 11 of ref 23. We avoided this situation by using high substrate concentrations and rather larger microelectrode−support distances. Although the less pronounced distance dependence of the GC mode limits the lateral resolution, larger working distances are more convenient for analytical purposes because of the reduced risk of pushing away the bead agglomerations by the insulating shielding of the microelectrode.

CONCLUSION

Biochemically active microstructures can be assembled on hydrophobic surfaces on the basis of magnetic attraction between paramagnetic, surface-modified beads in a droplet of bead suspension and a magnet held beneath the receiving surface. Their size is varied easily by the number of beads in the droplet used for deposition, and they are mechanically stable after drying. The biochemical activity can be restored by immersing them in a buffer. Images could be obtained at comparatively large working distances in the GC mode which is an advantage for sensing applications as it reduces the required vertical positioning accuracy for assay arrangements. Feedback images of streptavidin-coated beads were recorded after incubation of the beads with GOx. Despite the superior lateral resolution, the feedback mode seems less appropriate for assay configurations because of the more critical dependence on the working distance compared with that of the GC experiments. The high level of background current limits the sensitivity of this approach.

ACKNOWLEDGMENT

The authors thank Dr. Gerald Wagner (University of Leipzig, Institute of Mineralogy, Crystallography and Material Science) for providing the SEM images. Financial support was provided by DARPA Grant no. AFOSR-F30602-97-2-0102 and by Deutsche Forschungsgemeinschaft (Wi 1617/1-1). C.A.W. is Laws Fellow of the Department of Chemistry, University of Cincinnati.

Received for review August 25, 1999. Accepted November 4, 1999.

AC990977Q